Research Journal of Applied Sciences, Engineering and Technology 8(4): 530-540, 2014
DOI:10.19026/rjaset.8.1002
ISSN: 2040-7459; e-ISSN: 2040-7467

Submitted: March 29, 2014 Accepted: April 28, 2014 Published: July 25, 2014

Research Article

Hybrid Concatenated Super-orthogonal Space-time Frequency Trellis Coded MIMO-OFDM Systems

Ilesanmi B. Oluwafemi and Stanley H. Mneney
School of Engineering, University of KwaZulu-Natal, Durban, South Africa

Abstract: In this study, we propose two hybrids concatenated Super-Orthogonal Space-Time Trellis Codes (SOSTTC) applying iterative decoding in Orthogonal Frequency Division Multiplexing (OFDM) over frequency selective fading channels. The coding scheme is based on the concatenation of convolution coding, interleaving and space-time coding along multiple-transmitter/multiple-receiver diversity systems. The Pair wise Error Probability (PEP) for the two proposed concatenated schemes is derived and their performance is evaluated using computer simulation with Maximum a Posteriori (MAP) iterative decoding algorithm. Simulation results based on the iterative decoding process show a significant improvement in the achieved error rate performance of the concatenated scheme over existing concatenated designs.

Keywords: Concatenated codes, frequency selective fading channels, iterative decoding, orthogonal frequency division multiplexing, space-time decoding

INTRODUCTION

Employing multiple transmit and/or receive antennas in a communication system is an effective method of increasing the information capacity gain of a wireless communication system (Telatar, 1999; Foschini and Gans, 1998). Space-Time Coding (STC) proposed by Tarokh *et al*. (1998) combines channel coding, modulation, transmit diversity and/or receive diversity to guarantee a power and bandwidth efficient method of communication over fading channels. Super-Orthogonal Space-Time Trellis Code (SOSTTC) is a recently introduced STC scheme that combine set partitioning and a super set of orthogonal block codes in a systematic way, in order to provide full diversity and improved coding gain when compared with the earlier Space-Time Trellis Code (STTC) constructions (Jafarkhani and Sashadri, 2003; Siwamogsatham and Fitz, 2002; Bale *et al*., 2007; Hartling *et al*., 2008).

STCs are designed for a target diversity gain in a flat fading channel and they have been shown to suffer irreducible error floor in a frequency selective fading channel as a result of inter symbol interference (Aksoy and Aygolu, 2007). To improve the performance of STC in wideband frequency selective fading channels, two techniques have been proposed in literatures which are the use of orthogonal frequency division multiplexing and multichannel equalization (Sokoya and Maharaj, 2008, 2010). Multichannel equalization is said to have a setback of receiver complexity which gives OFDM an edge in resolving the problem of ISI. In an OFDM system, a high rate data stream becomes multiple low rate data streams in parallel over a number of orthogonal subcarriers (Shu-Ming and Yu-Shun, 2011; Hassan *et al*., 2011). OFDM system uses a Cyclic Prefix (CP) of length that is longer than the delay spread of channel impulse response to efficiently avoid the effect ISI (Yu *et al*., 2012; Huang *et al*., 2011) and offers a high performance in physical layer and serves as a fascinating multicarrier scheme for many wireless networks (Shaowei *et al*., 2012).

Turbo coding, which is a parallel concatenation of convolution codes, resulted in an unprecedented performance of a few tenths of a dB in the capacity of the Additive White Gaussian Noise (AWGN) channels (Berrou *et al*., 1993). Turbo codes employ a suboptimal, yet powerful iterative decoding algorithm whereby extrinsic information is exchanged between constituent codes. The astonishing performance of turbo codes demonstrated the great potential of concatenated coding schemes and resulted in the introduction of many other concatenated schemes employing the turbo principle. The serial concatenated scheme was proposed by Benedetto and Montorsi (1998) while Benedetto *et al*. (1997, 1998) proposed a double concatenated scheme with constituent convolutional codes.

STCs are designed to achieve maximum diversity but do not achieve high coding gain. In order to improve the coding gain of STC various concatenated schemes have been proposed (Lin and Blum, 2000; Tujkovic, 2000a; Gulati and Narayanan, 2003; Firmanto *et al*., 2002; Altunbaş and Yongacoglu, 2003; Gong and Letaief, 2000). Guidelines for the selection of

Corresponding Author: Ilesanmi B. Oluwafemi, School of Engineering, University of KwaZulu-Natal, Durban, South Africa

constituent codes of concatenated scheme involving STTC and convolutional codes are given by Lin and Blum (2001), while Byers and Takawira (2002) proposed the double concatenated scheme. The scheme presented by Su and Geraniotis (2002) involves parallel concatenation of STTCs in flat fading channels. Other concatenations involving SOSTTC and convolutional codes were presented by Altunbaş (2007) and Pillai and Mneney (2006) over flat Rayleigh fading channels. In frequency selective fading channels, convolutional codes were concatenated serially with STTC in OFDM systems in Patcharamaneepakor *et al*. (2003).

Motivated by the good performance of a double concatenated scheme presented in Benedetto *et al*. (1997) and the results of a hybrid concatenated topology in Bon-Jin *et al*. (2004), two concatenated schemes are proposed in order to further improve the coding gain of concatenated SOTTC-OFDM systems. The two schemes combine the field of turbo coding and super orthogonal space-time coding with OFDM technology. The first consists of a serial concatenation of a Parallel Concatenated convolutional code with a SOSTTC (PC-SOSTTC-OFDM) scheme and the second involves parallel concatenation of two serially concatenated convolutional and SOSTTC codes in OFDM systems (HC-SOSTTC-OFDM). The systems have the advantage of achieving diversity gain by exploiting all available diversity resources while high coding gain is guaranteed by the concatenations. The Frame Error Rate (FER) performance of the system is evaluated by computer simulations. We considered rate 2/3 recursive and non recursive convolutional codes for both the HC-SOSTTC-OFDM and the PC-SOSTTC-OFDM systems. A 16-state SOSTTC is considered as the inner code for the concatenations.

MATERIALS AND METHODS

System model:

Channel model: Consider a MIMO-OFDM system consisting of two transmit and M_R receive antennas. Each transmit antenna employs an OFDM modulator with K subcarriers. We assume no spatial correlation exists between the antennas and that the receiver has perfect knowledge of the channel while the transmitter does not know the channel. The Channel Impulse Response (CIR) between the transmit antenna p and receive antenna q with W independent delay paths on each OFDM symbol and an arbitrary power delay profile can be expressed as (Jafarkhani, 2005):

$$h_{p,q}(t) = \sum_{w=0}^{W-1} \alpha_{p,q}(w)\delta(t-\tau_w) \quad (1)$$

where, τ_w is the w^{th} path delay and $\alpha_{p,q}(w)$ is the fading coefficients at delay τ_w. Note that each $\alpha_{p,q}(w)$ is a complex Gaussian random variable with zero mean and variance $\sigma^2_w/2$ on each dimension. We assume that $\sum_{w=0}^{W} \sigma_w^2 = 1$ for normalization purposes in each of the transmit-receive links.

The Channel Frequency Response (CFR), that is the fading coefficient for the k^{th} subcarrier between transmit antenna p and receive antenna q with proper cyclic prefix and a perfect sampling time, is given by:

$$H_{p,q}(k) = \sum_{w=0}^{W-1} \alpha_{p,q}(w) e^{-j2\pi m\Delta_f \tau_w} \quad (2)$$

where, Δ_f is the inter-subcarrier spacing, $\tau_w = wT_s$ is the w^{th} path delay and $T_s = \frac{1}{K\Delta_f}$ is the sampling interval of the OFDM system. Assuming that the channel remain constant during an OFDM frame, the channel response becomes independent from the time variable t for a single symbol period and then the signal received by the q^{th} antenna ($1 \le q \le M_R$) at the nth symbol interval ($1 \le n \le N_x$) where, N_x is time interval, for the k^{th} subcarrier ($0 \le k \le K$-1) can be expressed as:

$$r_q^n(k) = \sum_{p=1}^{M_T=2} c_p^n(k) H_{pq}(k) + \mathrm{N}_q^n(k) \quad (3)$$

where,

M_T : The transmit antenna

$N^n_q(k)$: A circularly symmetric Gaussian noise term, with zero-mean and variance N_0 at n^{th} symbol period

Encoder structure:

Parallel Concatenated SOSTTC-OFDM (PC-SOSTTC-OFDM): The block diagram of the PC-SOSTTC-OFDM system is shown in Fig. 1 where the input bits are encoded by Convolutional Code 1 (CC1) as well as by Convolutional Code 2 (CC2) after interleaving by π_p. All the output bits from CC1 and CC2 are converted to a single serial stream. The serial stream is then interleaved by π_s and encoded by the SOSTTC to produce the complex symbols. The serial complex data are converted to parallel streams upon which IFFT is performed. Cyclic Prefix (CP) is then added to the transformed symbol before they are transmitted from each of the antenna. All the encoders are terminated using appropriate tail bits.

Hybrid Concatenated SOSTTC-OFDM systems (HC-SOSTTC-OFDM): The encoder block diagram of the proposed hybrid concatenated scheme is shown in Fig. 2 and it consists of a parallel concatenation of two serially concatenated schemes. Each of the serial concatenated schemes consists of an outer

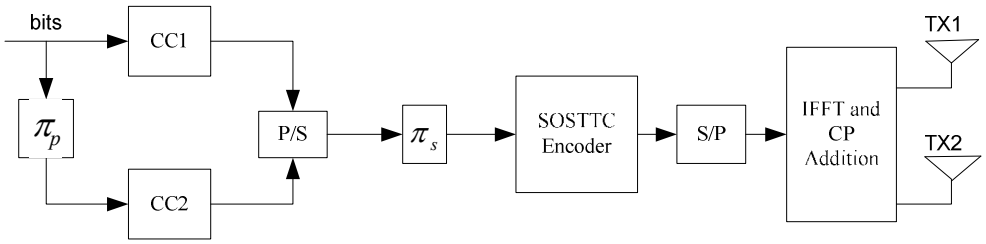

Fig. 1: Encoder block diagram of PC-SOSTTC-OFDM system

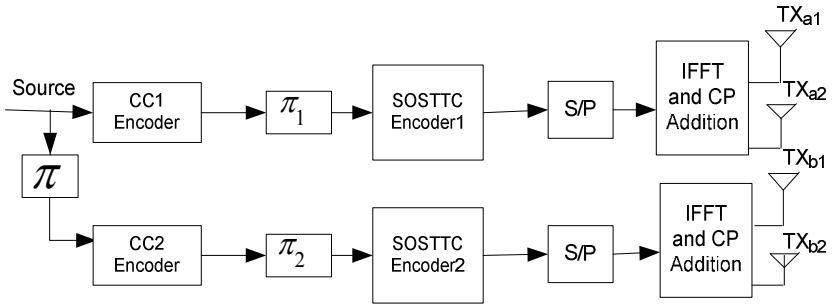

Fig. 2: Encoder block diagram of HC-SOSTTC-OFDM system

convolutional code concatenated via an interleaver with an inner SOSTTC. In the system, a block of N independent bits are encoded by the outer convolutional encoder of the upper serial part of the concatenated scheme. The output of the upper convolutional encoder is then passed through a random bit interleaver (π_1). The permuted bits from the interleaver are then fed to the upper SOSTTC encoder to generate a stream of complex data. The complex symbol from the SOSTTC encoder is thereafter converted to a parallel output and Inverse Fast Fourier Transform (IFFT) is performed on each of the parallel symbols. In order to avoid ISI caused by multipath delay, Cyclic Prefix (CP) is added to each of the transformed symbols before transmission from each of the antennas.

In the lower serial part of the encoding, the lower convolutional encoder receives the permuted version of the block of *N* independent bits and generates blocks of coded bits which are passed through another inter leaver π_2 to the lower SOSTTC encoder. It should be noted that the same convolutional code and SOSTTC used in the upper encoding is used in the lower encoder. The complex data from the output of the lower SOSTTC encoder are then converted to parallel outputs and an IFFT is performed on each of the parallel symbols. Cyclic Prefix (CP) is added to the transformed symbols before transmission from each of the antenna from the lower arm of the encoder. Note that each encoder is terminated using appropriate tail bits.

Decoder structure:

PC-SOSTTC-OFDM: A simplified block diagram of the PC-SOSTTC decoder is shown in Fig. 3. The symbol-by-symbol Maximum a Posteriori (MAP) decoder is used for the inner SOSTTC decoder and a bit-by-bit MAP decoder is used for the outer decoder. All the decoders used operate on the bit streams using the Soft-Input Soft-Output (SISO) algorithm, whereby extrinsic information is exchanged between the component decoders using soft estimates of their Log Likelihood Ratio (LLR) denoted as λ. This is performed with the presence of feedback loops that are provided. The four ports of the SISO system are used in the iterative decoding of the two outer decoders in order to fully exploit the potentials of the A Posteriori Probability (APP) algorithm. The subscript k which is the subcarrier index of λ is dropped for simplicity of description and the subscript of c and u will specify the decoder where st is used for the SOSTTC encoder, 1 for convolutional encoder CC1 and 2 for convolutional encoder CC2.

The inserted CP is first removed from the symbol and Fast Fourier Transform (FFT) is performed on each of them. The parallel data streams are then converted to serial symbols. On the first iteration, the SISO inputs $\lambda(u_{st}, I)$, $\lambda(u_1, I)$ and $\lambda(u_2, I)$ are all set to zero since no a priori information is available. By dropping the subcarrier index *k* for simplicity, the coded intrinsic LLR for the SOSTTC symbol-by-symbol SISO $\lambda(c_{st}, I)$ module is computed as (4):

$$\lambda(c_{st},I)=-\frac{1}{2\sigma^2}\sum_{q=1}^{M_R}\left|r-\sum_{p=1}^{M_T}H_{pq}c\right|^2+\frac{1}{2\sigma^2}\sum_{q=1}^{M_R}\left|r-\sum_{p=1}^{M_T}H_{pq}c_0\right|^2 \quad (4)$$

where,

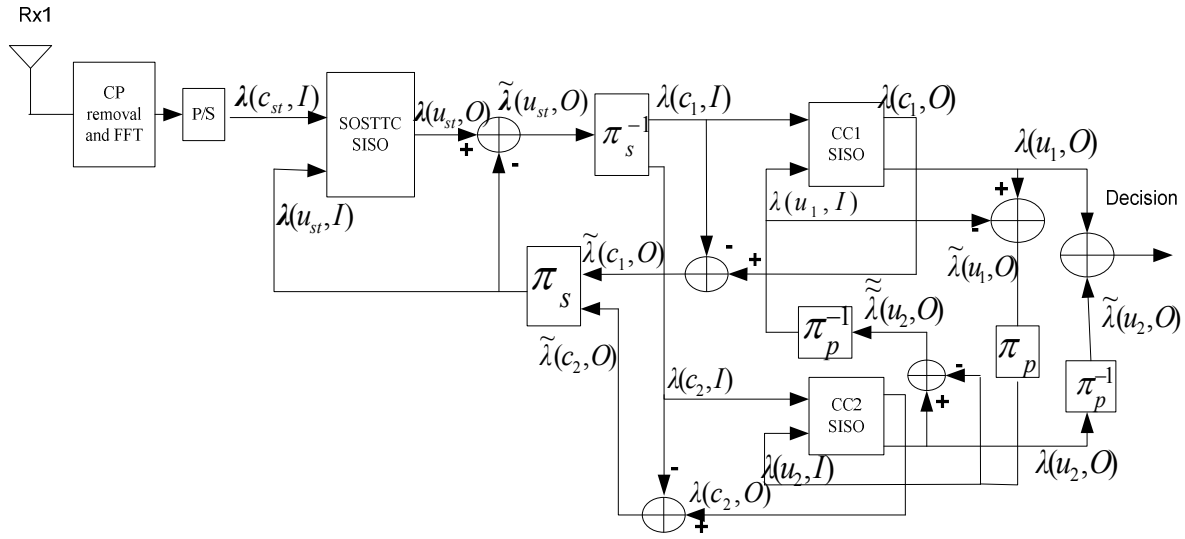

Fig. 3: The block diagram of the PC-SOSTTC-OFDM decoder

σ^2 = The variance of the independent complex Gaussian noise variable

c_0 = The reference symbol and c is one of the possible output symbol

The extrinsic LLR for the SOSTTC-SISO is then calculated as:

$$\tilde{\lambda}(u_{st}, O) = \lambda(u_{st}, O) - \lambda(u_{st}, I) \quad (5)$$

where, u, O, I denotes un-coded information, extrinsic and a priori respectively.

This extrinsic LLR is then passed to the inverse inter leaver π_s^{-1} from where the information pertaining to the coded bits of CC1 and CC2, λ (c_1, I) and λ (c_2, I), respectively are extracted. Then the output LLRs λ (c_1, O) and λ (u_1, O) are calculated by the CC1-SISO. The LLR λ (u_1, I) is subtracted from λ (u_1, O) to obtain the LLR $\tilde{\lambda}(u_1, O)$ which is then passed through the inter leaver π_p to obtain the intrinsic information λ (u_2, I) for the CC2-SISO.

The output LLRs λ (c_2, O) and λ (u_2, O) are also calculated by the CC2-SISO. The LLR λ (u_2, I) is subtracted from λ (u_2, O) to obtain the LLR $\tilde{\lambda}(u_2, O)$ which is then passed through the de-inter leaver π_p^{-1} to obtain the intrinsic information λ (u_1, I) for the CC1-SISO. A single LLR stream constructed from $\tilde{\lambda}(c_2, O)$ and $\tilde{\lambda}(c_1, O)$ is interleaved by π_s to become λ (u_{st}, I) on the next iteration. The process is iterated for several times. On the final iteration, the LLR λ (u_2, O) is de-interleaved π_p^{-1} to obtain $\tilde{\lambda}(u_2, O)$ which is added to λ (u_1, O) upon which the decision device acts to determine the input bits.

HC-SOSTTC-OFDM decoder: The decoding block diagram of the iterative decoding system of the HC-SOSTTC-OFDM system is shown in Fig. 4. The subscript of the c and u specifies the decoder where st1 is used for the upper SOSTTC encoder, st2 for the lower SOSTTC encoder, 1 for the upper convolutional code and 2 for the lower convolutional code. The decoder consists of two serial parts and one parallel sector. For the upper serial decoding, the inserted CP is first removed from each of the symbols and FFT is performed on each of the symbols. The parallel streams are then converted to serial symbols and the coded intrinsic LLR for the SOSTTC symbol-by-symbol SISO module is computed as in (4).

The SOSTTC SISO takes the intrinsic LLR λ (c_{st1}, I) and the a priori information from the CC1 SISO which is initially set to zero and computes the extrinsic LLR given as:

$$\tilde{\lambda}(u_{st1}, O) = \lambda(u_{st1}, O) - \lambda(u_{st1}, I) \quad (6)$$

where, u, O, I denotes un-coded information, extrinsic and a priori, respectively.

The extrinsic information is de-interleaved (π_1^{-1}) and fed to the CC1-SISO to become its a priori information. The a priori information is then fed to the CC1-SISO together with the un coded a priori information from the parallel part to compute the extrinsic information for the CC1-SISO. The A Posteriori Probability (APP) output of the upper bit-by-bit MAP consists of the extrinsic $\tilde{\lambda}(c_1, O)$) and a priori LLR given as:

$$\tilde{\lambda}(c_1, O) = \lambda(c_1, O) - \lambda(c_1, I) \quad (7)$$

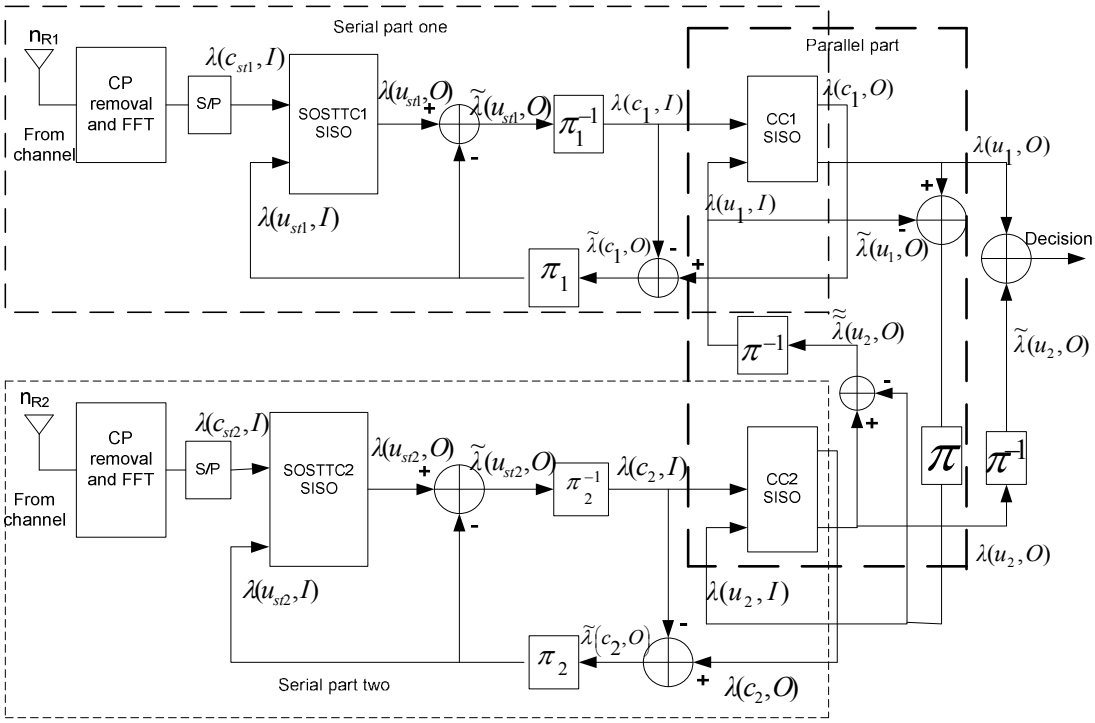

Fig. 4: The decoder block diagram of the HC-SOSTTC-OFDM system

where, c is the coded information, O is extrinsic and I is Intrinsic information. The APP outputs of the MAP decoders of the lower serial part 2 can be obtained by changing index 1 in (6) and (7) to index 2.

The parallel interconnection component of the iterative decoding process is described by (8) and (9):

$$\tilde{\lambda}(u_1, O) = \lambda(u_1, O) - \lambda(u_1, I) \quad (8)$$

$$\tilde{\lambda}(u_2, O) = \lambda(u_2, O) - \lambda(u_2, I) \quad (9)$$

The process is iterated for several times and the decision device chooses the bit with the maximum APP in the last iteration using the summed values of the output LLRs of both the upper and lower bit-by-bit MAP decoders.

Component codes:

Inner code: The SOSTTC code with the transmission matrix given as (10) is considered as the inner codes (Jafarkhani and Sashadri, 2003):

$$C(x_1, x_2, \theta) = \begin{pmatrix} x_1 e^{j\theta} & x_2 \\ -x_2^* e^{j\theta} & x_1^* \end{pmatrix} \quad (10)$$

where, x_1 and x_2 are selected by input bits. The first row corresponds to the symbols transmitted in time slot 1, the second row, to the symbols transmitted in time slot 2. The first column corresponds to the symbols transmitted by antenna 1 while the second column corresponds to the symbols transmitted by antenna 2. The value of θ is picked such that for any choice of x_1 and x_2 from the original constellation point, the resulting transmitted signals are also from the same constellation (Jafarkhani and Sashadri, 2003). For M-Phase Shift Keying (PSK) modulation with constellation signal represented by $x_i \in e^{j2\pi a/M}$, $i = 1, 2$, $a = 0, 1, \ldots, M\text{-}1$, one can pick $\theta = 2\pi a'/M$, where $a' = 0, 1, \ldots, M\text{-}1$ to avoid constellation expansion and the resulting transmitted signal are also members of the M-PSK constellation. Since the transmitted signals are from a PSK constellation, the peak-to-average power ratio of the transmitted signal is equal to one. Specifically, the choice of θ that can be used in (10) is given as 0, π and 0, π/2, π, 3π/2 for Binary Phase Shift Keying (BPSK) and Quaternary Phase Shift Keying (QPSK) respectively (Jafarkhani and Sashadri, 2003; Aksoy and Aygolu, 2007; Birol and Aygölü, 2008). SOSTTC were designed for quasistatic fading channels based on the rank and determinant criteria and their trellis structure have a large number of parallel transitions. Hence, their error performance breaks down when used in wideband channels. To achieve multipath diversity with SOSTTC, parallel transitions must be avoided and to avoid the parallel transition constraint, for a rate b bits/sec/ Hz, at least M^2

Table 1: Generating matrices for the outer codes

Code description	G (D)	Min. hamming distance
4 states rate 2/3 NRC	$\begin{bmatrix} 1+D, & D, & 1 \\ 1+D, & 1, & 1+D \end{bmatrix}$	3
4 states rate 2/3 RSC	$1,\ 0,\ \frac{1+D^2}{1+D+D^2}$	
	$0,1,\ \frac{1+D}{1+D+D^2}$	3

Min.: Minimum

states are needed in the trellis structure of SOSTTC (Sokoya and Maharaj, 2010). We considered the 16-state SOSTTC presented by Oluwafemi and Mneney (2013) for this study.

Outer codes: Convolutional codes are considered as the outer codes. We considered both recursive systematic and non recursive codes. The generator matrices of the outer codes considered for our investigation are given in Table 1.

Pairwise error probability analysis: The Pair wise Error Probability (PEP) presented in Tujkovic (2000b) is herewith extended for the analysis of the two proposed schemes in this section. Assumed that the symbol matrix sequence $\mathbf{C} = \{c[1],..., c(L)\}$ is transmitted where L is the trellis path length chosen to be smaller than K and the Maximum Likelihood (ML) decoder decided in favor of coded sequence $\hat{\mathbf{C}} = \{\hat{c}[1],...,\hat{c}(L)\}$, if $m(r,\hat{\mathbf{C}}) \geq m(r,\mathbf{C})$, where $m(r,\hat{\mathbf{C}})$ is the ML metric related to the decoded path given by:

$$m(r,\hat{\mathbf{C}}) = \sum_{l=1}^{L}\sum_{n=1}^{N_x}\sum_{q=1}^{M_R}\left| r_q^n(k) - \sum_{p=1}^{M_T} H_{pq}(l)\hat{c}_p^q(l)\right|^2 \quad (11)$$

And $m(r, C)$ is the ML metric for the correct path given as:

$$m(r,\mathbf{C}) = \sum_{l=1}^{L}\sum_{n=1}^{N_x}\sum_{q=1}^{M_R}\left| r_q^n(k) - \sum_{p=1}^{M_T} H_{pq}(l)c_p^q(l)\right|^2 \quad (12)$$

Thus the PEP is given as:

$$\mathbf{P}((\mathbf{C}\to\hat{\mathbf{C}})\,|\,\mathbf{H}) = P_r[m(r,c) - m(r,\hat{c}) > 0\,|\,\mathbf{H}] \quad (13)$$

Substituting (11) and (12) in (13) and simplifying in term of Gaussian Q-function yields:

$$\mathbf{P}((\mathbf{C}\to\hat{\mathbf{C}})\,|\,\mathbf{H}) = Q\left(\sqrt{\frac{E_s}{2N_0}D}\right) \quad (14)$$

where,

N_0 : The variance of the noise

E_s : The symbol energy and D is defined as:

$$D = \sum_{q=1}^{M_R}\sum_{l=1}^{L}\sum_{n=1}^{N_x} D_n^q(l),$$

where,

$$D_n^q(l) = \left|\sum_{p=1}^{M_T}[c_p^n(l) - \hat{c}_p^n(l)]H_{pq}(l)\right|^2.$$

Using an upper bound for the Q-function $Q(x) \leq 1/2e^{-x^2/2}$, PEP can be upper bounded as:

$$\mathbf{P}((\mathbf{C}\to\hat{\mathbf{C}})\,|\,\mathbf{H}) \leq \frac{1}{2}\exp\left(-\frac{E_s}{4N_0}D\right) \quad (15)$$

Since the expected value of $H_{pq}(l)$ is zero for all $H_{pq}(l)$'s, then the expected value of $D^q{}_n(l)$ is given as:

$$E[D_n^q(l)] = \sum_{p=1}^{M_T} E[|\,c_p^n(l) - \hat{c}_p^n(l)\,|^2\,|\,H_{pq}(l)\,|^2]$$

The PEP upper bound average over all possible channel realizations is given from (15) as:

$$\begin{aligned}&\mathbf{P}(\mathbf{C}\to\hat{\mathbf{C}}) = \mathbf{E}[\mathbf{P}((\mathbf{C}\to\hat{\mathbf{C}})\,|\,\mathbf{H})]\\ &\leq \prod_{q=1}^{M_R}\prod_{p=1}^{M_T}\prod_{l=1}^{L} E\left\{\frac{1}{2}\exp\left[\frac{-E_s}{4N_0}\left(\sum_{n=1}^{N_x}|\,c_p^n(l) - \hat{c}_p^n(l)\,|^2\,|\,H_{pq}(l)\,|^2\right)\right]\right\}\end{aligned} \quad (16)$$

For all $\upsilon \in \Re$:

$$E[\exp(\nu\varsigma^2)] = \int_0^\infty 2\varsigma\exp(-\varsigma^2)\exp(\nu\varsigma^2)d\varsigma = \frac{1}{1-\nu}, \quad (17)$$

where, ς is a random variable with Rayleigh distribution with variance ½. Taking $\varsigma = H_{pq}(l)$ in (17) and assuming that they are independently-complex Gaussian-distributed random variable, then (16) yields:

$$\begin{aligned}&\mathbf{P}(\mathbf{C}\to\hat{\mathbf{C}}) \leq \prod_{q=1}^{M_R}\prod_{p=1}^{M_T}\prod_{l=1}^{L}\frac{1}{1+\frac{E_s}{4N_0}\sum_{n=1}^{N_x}|\,c_p^n(l) - \hat{c}_p^n(l)\,|^2}\\ &\leq \prod_{q=1}^{M_R}\prod_{p=1}^{M_T}\prod_{l\in\eta}\frac{1}{1+\frac{E_s}{4N_0}\sum_{n=1}^{N_x}|\,c_p^n(l) - \hat{c}_p^n(l)\,|^2}\end{aligned} \quad (18)$$

where, η is the set of all l for which $c_p^n(l) \neq \hat{c}_p^n(l)$. Denoting the number of elements in η by l_η, then at high signal to noise ratio, Eq. (18) can be expressed as:

$$\mathbf{P}(\mathbf{C} \to \hat{\mathbf{C}}) \le \frac{1}{\left[\left(\frac{E_s}{4N_0}\right) d_p(l_\eta)\right]^{M_R}} \tag{19}$$

where,

$$d_p(l_\eta) = \prod_{l}^{L} \prod_{p=1}^{M_T} \prod_{n=1}^{N_s} \left| c_p^n(l) - \hat{c}_p^n(l) \right|^2$$

is the product sum distance along the error events $\mathbf{P}(\mathbf{C} \to \hat{\mathbf{C}})$ path and l_η is called the effective length of this error event. The built-in frequency diversity of the SOSTTC is calculated as L_η = min (l_η) while the product sum distance is calculated as $d_p(L_\eta)$ = min [dp (l_η)].

Assuming that the whole codeword of each arm of the HC-SOSTTC-OFDM $\mathbf{X}$ is constructed from N_η different $\mathbf{C}$ sequence denoted by C_η for η = 1,…., N_η so that $\mathbf{X} = C_1, ..., C_\eta ..., C_{N\eta}$. Then:

$$\mathbf{P}(\mathbf{X} \to \hat{\mathbf{X}}) = \prod_{\eta=1}^{N_\eta} \mathbf{P}(\mathbf{C}_\eta \to \hat{\mathbf{C}}_\eta) \le \frac{1}{\left[\left(\frac{E_s}{4N_0}\right)^{l_\gamma(\mathbf{X},\hat{\mathbf{X}})} d_p(l_\gamma)\right]^{M_R}} \tag{20}$$

where, $l_r(X, \hat{X})$ is the effective length given as:

$$l_\gamma(\mathbf{X}, \hat{\mathbf{X}}) = \sum_{\eta=1}^{N_\eta} l_\eta(\mathbf{C}_\eta, \hat{\mathbf{C}}_\eta)$$

And $d_p(l_r)$ is the product sum distance defined as:

$$d_p(l_\gamma) = \prod_{\eta=1}^{N_\eta} d_p(l_\eta).$$

The space-frequency diversity of each arm of the HC-SOSTTC-OFDM scheme is therefore calculated from:

$$L_\gamma = \min(l_\gamma) \tag{21}$$

The design criteria from (20) at high signal-to-noise ratio involve maximization of the build-in-space-frequency diversity of the concatenated code and the minimum product sum distance. Maximization of the build-in-space-frequency diversity of the concatenated code optimizes the diversity while the maximization of the minimum product sum distance optimizes the coding gain of the concatenated scheme.

If we assume that the bit inter leaver maps different bits of the outer coded bit vector pairs into different groups, then the minimum number of different groups in a pair will be equal to the free distance d_{free} of the outer code. With this assumption, the build-in space-frequency diversity of each arm of the HC-SOSTTC-OFDM becomes $L_r = L_\eta\, d_{free}$ (outer code).

The diversity of each arm of the HC-SOSTTC-OFDM concatenated code from (20) and (21) can then be written as:

$$D_g = M_R \times \min\{L_\eta d_{free}(outercode), M_T W\} \tag{22}$$

From (22) the overall diversity of the HC-SOSTTC-OFDM can be written as:

$$D_g(Total) = 2 \times M_R \times \min\{L_\eta d_{free}(outer\ code), M_T W\}, \tag{23}$$

where,

$$d_{free}(outercode) = d_{free}(CC1) or\ d_{free}(CC2)$$

For the PC-SOSTTC-OFDM system, the build-in space-frequency diversity is $L_r = L_\eta d_{free}$ (outer code). The overall diversity of the PC-SOSTTC-OFDM concatenated code is given by (22) but the d_{free} is the resultant d_{free} of the parallel concatenated convolutional code given as:

$$d_{free}(outercode) = d_{free}(CC1) + d_{free}(CC2)$$

RESULTS AND DISCUSSION

In this section, simulation results illustrating the performance of the proposed concatenated scheme over frequency selective fading channels are provided. For the simulation, we considered a MIMO-OFDM concatenated scheme equipped with two transmit antennas and one/or two receive antennas. Each of the OFDM modulator utilizes 64 subcarriers with a total system bandwidth of 1 MHz and FFT duration of 80 μs. The system's subcarrier spacing is 15 kHz with symbol duration of 64 μs while the guard band interval is 16 μs. The performance curves are described by means of Frame Error Rate (FER) versus the receive SNR with QPSK constellation. We simulate the system over two channel scenarios:

- A quasi-static channel with 2-paths uniform power delay profile. The delay between these paths is one OFDM sample duration.
- Typical Urban (TU) six paths COST 207 power delay profile reported in Digital Land Mobile Radio Communications (1989).

The channel is assumed constant over two symbol periods (frame) and changes independently over each frame. We also assume perfect channel state information at the receiver with perfect timing and frequency synchronization between the transmitter and the receiver.

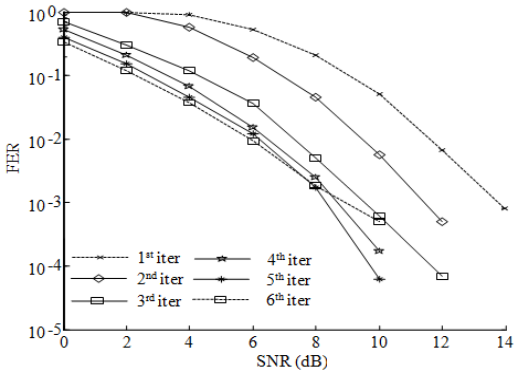

Fig. 5: FER performance of PC-SOSTTC-OFDM for various numbers of decoding iterations over the Typical Urban (TU) six-path COST 207 channel model

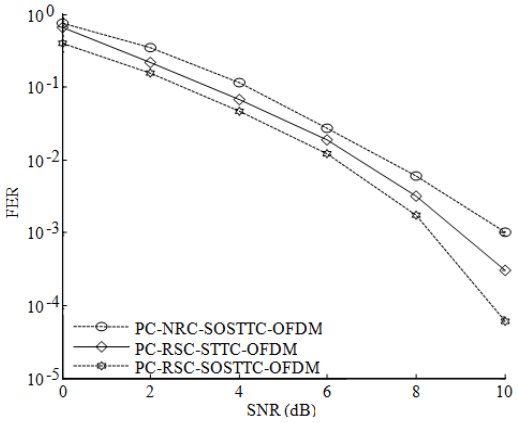

Fig. 6: FER performance of PC-NRC-SOSTTC-OFDM, PC-RSC-STTC-OFDM and PC-SOSTTC-OFDM over the Typical Urban (TU) six-path COST 207 channel model

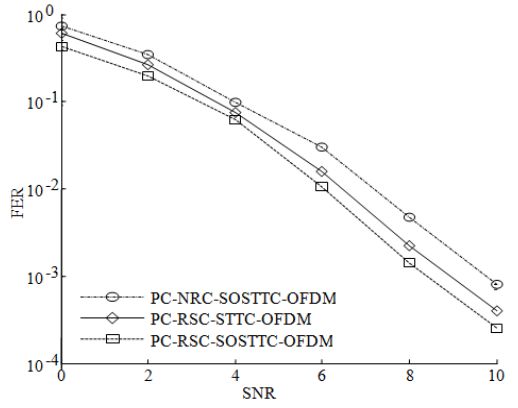

Fig. 7: FER performance of PC-NRC-SOSTTC-OFDM, PC-RSC-STTC-OFDM and PC-SOSTTC-OFDM over the two-ray channel model

For the PC-SOSTTC-OFDM, we used the 4-state rate-2/3 both recursive and non recursive convolutional code in Table 1 as the outer codes. The inbuilt space frequency diversity (L_η) of the SOSTTC used as the inner code for trellis path length L = 2 is 2. The code FER performance is evaluated for various numbers of iterations in Fig. 5. The rate 2/3 Recursive Systematic Convolutional (RSC) code is considered as the outer codes for this case. The coding gain achieved by the system is seen to increase as the number of decoding iterations increases and start saturating at the 4th iteration. The system however did not achieve the maximum diversity order as a result of inter leaver gain saturation (error floor). Error floor at higher SNR region is a peculiar characteristic of parallel concatenation scheme (Yu *et al*., 2012).

In Fig. 6 the FER performance of the PC-SOSTTC-OFDM is shown for both RSC and Non Recursive Convolutional (NRC) code outer codes and for inner STTC code with RSC outer code. The scheme with RSC outer code is seen to provide coding gain of about 0.6 and 1.6 dB when compared with its counterpart with STTC inner code and NRC outer code respectively. We also evaluate the FER performance of the PC-SOSTTC-OFDM in Fig. 7 using both the RSC and the NRC outer codes and compared it with PC-STTC-OFDM under the two ray channel model. Under this channel scenario, the scheme with RSC outer codes is observed from the FER performance curve to achieve full diversity order of 4 and also achieve additional coding gain of about 0.6 and 1.4 dB when compared with its counterpart with STTC inner code and NRC outer code respectively. The schemes with outer RSC codes achieve higher coding gain when compared with the scheme with NRC outer code because RSC benefit from interleaving gain in iterative decoding.

The same 4-state rate-2/3 recursive and non recursive convolutional codes in Table 1 are used as the outer code for the HC-SOSTTC-OFDM system. Each serial parts of the HC-SOSTTC-OFDM scheme employs 64 subcarriers.

The FER performance of the HC-SOSTTC-OFDM system is shown in Fig. 8 for various numbers of iterations using channel condition 1. From the FER performance curve, it can be observed that the HC-SOSTTC-OFDM achieve diversity order of 12 at the 6th iteration.

The FER performance of the system is presented for both RSC and NRC outer code in Fig. 9. In the same Fig. 9 we compare the FER performance with a case of STTC inner code. The scheme with RSC outer code provide additional coding gain of about 0.8 and 1.7 dB when compared with the scheme with the STTC inner code and NRC outer code system respectively. Figure 10 shows the FER for the HC-SOSTTC-OFDM system using the 2 rays channel model. It can be seen from the slope of the performance curve that HC-SOSTTC-OFDM with RSC outer code achieves full

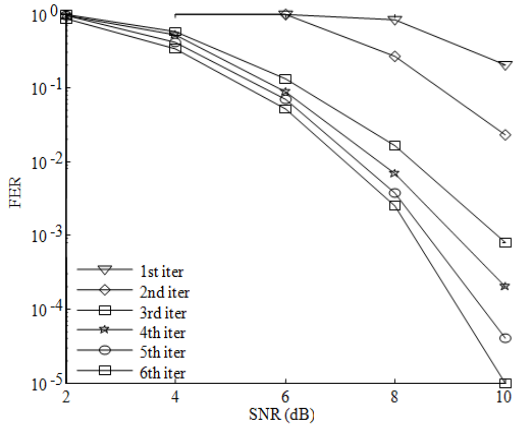

Fig. 8: FER performance of HC-SOSTTC-OFDM for various numbers of decoding iterations over the Typical Urban (TU) six-path COST 207 channel model

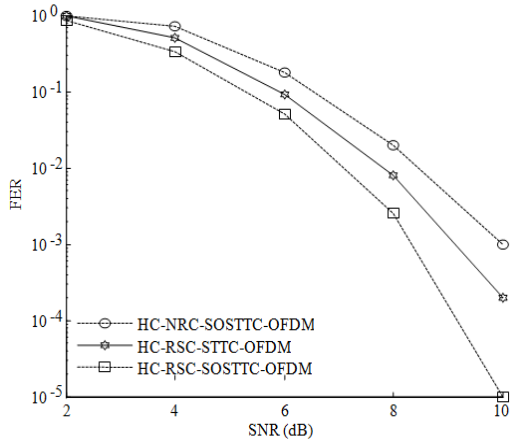

Fig. 9: FER performance of HC-NRC-SOSTTC-OFDM, HC-RSC-STTC-OFDM and HC-SOSTTC-OFDM over the Typical Urban (TU) six-path COST 207 channel model

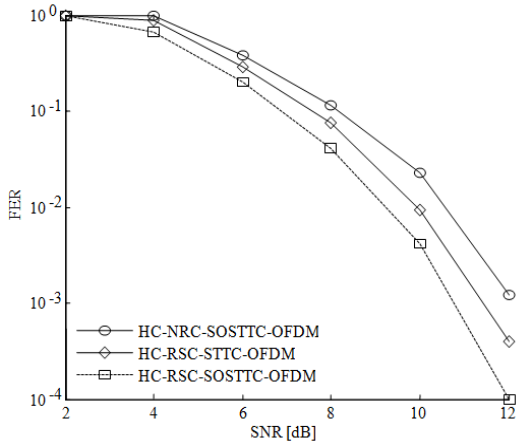

Fig. 10: FER performance of HC-NRC-SOSTTC-OFDM, HC-RSC-STTC-OFDM and HC-SOSTTC-OFDM over the two-ray channel model

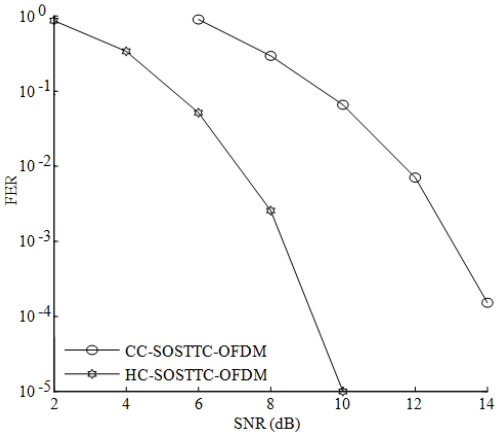

Fig. 11: FER performance comparison of CC-SOSTTC-OFDM and HC-SOSTTC-OFDM systems over the Typical Urban (TU) six-path COST 207 channel model

diversity order of 8 under this channel condition. We can also observe from the FER curve of Fig. 10 that the code with RSC outer codes achieves additional coding gain of about 1.3 and 0.6 dB when compared with the HC-SOSTTC-OFDM with NRC outer code and HC-STTC-OFDM system respectively.

Note that, to have the same number of symbols per frame and the same delay length for both systems, the number of OFDM subcarrier for the scheme with STTC inner code was selected as 128. In Fig. 11 we compare the FER performance of HC-SOSTTC-OFDM with that of CC-SOSTTC-OFDM from where it is observed that the HC-SOSTTC-OFDM achieved higher diversity order than the CC-SOSTTC-OFDM and also present additional coding gain of 5.0 dB but with double decoding complexity.

Decoding complexity: In this section, the relative estimated complexity of the proposed schemes in MIMO-OFDM systems is presented. The approach presented in Hanzo *et al*. (2002) is adopted in analyzing the complexity of the two proposed schemes. In computing the estimated complexity, the estimated complexity of the whole systems is assumed to depend only on the channel decoder, i.e., the complexity associated with the modulator, demodulator, STC encoder are assumed to be insignificant compared with the complexity of the channel decoders. The complexity of the channel decoders which depends directly on the number of trellis transitions per information data bit is used as the basis of comparison:

$$Comp(SOSTTC) = \frac{2^{BPS} \times No\ of states}{BPS} \quad (24)$$

For the concatenated schemes, the Log-MAP decoding algorithm for iterative decoding is applied. Since the Log-MAP algorithm has to perform forward as well as backward recursion and soft output

Table 2: Estimated decoder complexity of the proposed schemes

Scheme	Decoding algorithm	Complexity
CC-SOSTTC-OFDM	Log-map	1368
PC-SOSTTC-OFDM	Log-map	1584
HC-SOSTTC-OFDM	Log-map	2592

calculation, which results in traversing through the trellis three times, the number of trellises in Log-MAP decoding algorithm is assumed to be three times higher than the conventional Viterbi Algorithm.

For the rate-2/3, 4-state CC decoder, the complexity is estimated as:

$$Comp(CC\{3,2,K\}) = 3 \times 2^{K-1} \times 3 \times no\ of\ \ iterations \quad (25)$$

where, K is the constraint length of convolutional code.

For SOSTTC in the iterative decoding, the complexity is estimated as:

$$Comp\{SOSTTC_{iter}\} = \frac{3 \times 6 \times 2^{BPS} \times No\ of\ \ states}{BPS} \quad (26)$$

Applying Eq. (25) and (26) and considering six iterations for all the concatenated schemes, the estimated decoding complexity for all the proposed schemes in OFDM systems is summarized in Table 2. Here, it is explicitly assumed that 256 bits are needed for the 64 subcarriers without the tail bits. It is obvious from Table 2 that the diversity advantage and the high coding gain provided by the concatenated schemes comes with higher decoding complexity.

CONCLUSION

In this study, two concatenated schemes with constituent codes of convolutional and SOSTTC codes are proposed for MIMO OFDM systems. The first consists of a serial concatenation of a parallel concatenated convolutional code with a SOSTTC and the second involves parallel concatenation of two serially concatenated convolutional and SOSTTC codes in OFDM systems. The concatenated schemes in MIMO-OFDM systems have the advantage of achieving high diversity gain by exploiting available diversity resources and high coding gain is provided by the concatenations. The PEP is derived for the two schemes and the systems FER performance with Maximum a Posteriori (MAP) iterative decoding algorithm is presented by computer simulations. We showed that the diversity order of the concatenated schemes depends on the inbuilt diversity order of the SOSTTC inner code and the minimum hamming distance d_{free} of the outer convolutional code.

ACKNOWLEDGMENT

The authors are indebted to Center for Engineering Postgraduate Study (CEPS), University of KwaZulu-Natal for the support made available for this study.

REFERENCES

Aksoy, K. and U. Aygolu, 2007. Super-orthogonal space-time frequency trellis coded OFDM. IET Commun., 1(3): 317-324.

Altunbaş, İ., 2007. Performance of serially concatenated coding schemes for MIMO systems. Int. J. Electron. Comm., 61: 1-9.

Altunbaş, İ. and A. Yongacoglu, 2003. Error performance of serially concatenated space-time coding. J. Commun. Netw., 3: 135-140.

Bale, M., B. Laska, D. Dunwell, F. Chan and H. Jafarkhani, 2007. Computer design of super-orthogonal space-time trellis code. IEEE T. Wirel. Commun., 6(2): 463-467.

Benedetto, S. and G. Montorsi, 1998. Serial concatenation of interleaved codes: Performance analysis, design and iterative decoding. IEEE T. Inform. Theor., 44(3): 909-926.

Benedetto, S., D. Divsalar, D. Montorsi and F. Pollara, 1997. A Soft-Input Soft-Output APP module for iterative decoding of concatenated codes. IEEE Commun. Lett., 1(1): 22-24.

Benedetto, S., D. Divsalar, D. Montorsi and F. Pollara, 1998. Analysis, design and iterative decoding of double serially concatenated codes with interleavers. IEEE J. Sel. Area. Comm., 16(2): 231-244.

Berrou, C., A. Glavieux and P. Thitimajshima, 1993. Near shannon limit error correcting coding and decoding: Turbo-codes. Proceedings of IEEE International Conference on Communications (ICC, 1993), 2: 1064-1070.

Birol, A. and Ü. Aygölü, 2008. Super-orthogonal space-time trellis codes for two transmit antennas in fast fading channel. Int. J. Commun. Syst., 21: 331-334.

Bon-Jin, K., C. Jong-Moon and K. Changeon, 2004. Analysis of serial and hybrid concatenated space-time codes applying iterative decoding. AEU-Int. J. Electron. Comm., 58(6): 420-423.

Byers, G.J. and F. Takawira, 2002. Double concatenated space-time trellis codes. Proceeding of IEEE AFRICON 6th Africon Conference in Africa, 1: 143-148.

Digital Land Mobile Radio Communications, 1989. Commission of the European Communities. COST 207, Luxembourg, Belgium.

Firmanto, W., Z. Chen, B. Vucetic and J. Yuag, 2002. Space-time turbo trellis coded modulation for wireless data communication. EURASIP J. Appl. Sig. P., 5: 459-470.

Foschini, G.J. and M.J. Gans, 1998. On limits of wireless communications in a fading environment when using multiple antennas. Wireless Pers. Commun., 6: 311-335.

Gong, Y. and K.B. Letaief, 2000. Analysis and design of trellis coded modulation with transmit diversity for wireless communications. Proceeding of IEEE Wireless Communication and Networking Conference (WCNC, 2000), pp:1356-1361.

Gulati, V. and K.R. Narayanan, 2003. Concatenated codes for fading channels based on recursive space-time trellis codes. IEEE T. Wirel. Commun., 2(1): 118-128.

Hanzo, L., T.H. Liew and B.L. Yeap, 2002. Turbo Coding,Turbo Equalization and Space-time Codes for Transmission in Fading Channels. 1st Edn., John Wiley and Sons, Chichster, England.

Hartling, E.R., F. Chan and H. Jafarkhani, 2008. Design rules for extended super-orthogonal space-time trellis codes. Proceedings of Canadian Conference on Electrical and Computer Engineering (CCECE, 2008), pp: 621-626.

Hassan, E.S., X. Zhu, S.E. El-Khamy, M.I. Dessouky, S.A. El-Dolil and F.E. Abd El-Samie, 2011. Performance evaluation of OFDM and single-carrier systems using frequency domain equalization and phase modulation. Int. J. Commun. Syst., 24: 1-13.

Huang, X.L., G. Wang and F. Hu, 2011. Minimal Euclidean distance-inspired optimal and suboptimal modulation schemes for vector OFDM system. Int. J. Commun. Syst., 24: 553-567.

Jafarkhani, H., 2005. Space-time Coding: Theory and Practice. 1st Edn., Cambridge University Press, Cambridge, pp: 152-167.

Jafarkhani, H. and N. Sashadri, 2003. Super-orthogonal space-time trellis codes. IEEE T. Inform. Theor., 49(4): 937-950.

Lin, X. and R.S. Blum, 2000, Improved space-time codes using serial concatenation. IEEE Commun. Lett., 4(7): 221-223.

Lin, X. and R.S. Blum, 2001. Guideline for serially concatenated space-time code design in flat Rayleigh fading channels. Proceeding of IEEE Signal Processing Workshop on Signal Processing Advances in Wireless Communications, pp: 247-250.

Oluwafemi, I.B. and S.H. Mneney, 2013. Improved super-orthogonal space-time trellis coded MIMO-OFDM system. IETE J. Res., 59(6): 665-671.

Patcharamaneepakor, P., R. Rajathera and K. Ahmed, 2003. Performance analysis of serial concatenated space-time code in OFDM over frequency selective channel. Proceedings of IEEE Vehicular Technology Conference (VTC, 2003), pp: 746-750.

Pillai, J.N. and S.H. Mneney, 2006. Turbo decoding of super orthogonal space-time trellis codes in fading channels. Wireless Pers. Commun., 37: 371-385.

Shaowei, W., H. Fangjiang, Y. Mindi and D. Sidan, 2012. Resource allocation for multiuser cognitive OFDM networks with proportional rate constraints. Int. J. Commun. Syst., 25: 254-269.

Shu-Ming, T. and H. Yu-Shun, 2011. A novel ICI self-cancellation scheme for OFDM systems. Int. J. Commun. Syst., 24: 1496-1505.

Siwamogsatham, S. and P. Fitz, 2002. Improved high-rate space-time codes via concatenation of expanded orthogonal block code and M-TCM. Proceeding of IEEE International Conference on Communication (ICC, 2002), pp: 636-640.

Sokoya, O. and B.T. Maharaj, 2008. Performance of space time coded orthogonal frequency division multiplexing schemes with delay spreads. Proceedings of the 14th IEEE Mediterranean IEEE Electrotechnical Conference (MELECON, 2008), pp: 198-203.

Sokoya, O. and B.T. Maharaj, 2010. Super-orthogonal block code with channel equalization and OFDM in frequency selective fading. EURASIP J. Wirel. Comm., Article ID 10.1155:153846.

Su, H.J. and E. Geraniotis, 2002. Space-time turbo codes with full antenna diversity. IEEE T. Commun., 49(1): 47-57.

Tarokh, V., N. Seshadri and A.R. Calderbank, 1998. Space-time codes for high data rate wireless communication: Performance criterion and code construction. IEEE T. Inform. Theor., 44: 744-765.

Telatar, E., 1999. Capacity of multi-antenna gaussian channels. Eur. T. Telecommun., 10(6): 585-595.

Tujkovic, D., 2000a. Recursive space-time trellis codes for turbo coded modulation. Proceedings of IEEE Global Communications Conference (GLOBECOM, 2000), pp: 1010-1015.

Tujkovic, D., 2000b. Space-time turbo coded modulation. Proceedings of Finish Wireless Communication Workshop (FWCW, 2000), pp: 85-89.

Yu, J.L., C.H. Wu and M.F. Lee, 2012. MC-CDMA MIMO systems with quasi-orthogonal space-time block codes: Channel estimation and multiuser detection. Int. J. Commun. Syst., 25: 294-313.